Model of ion-induced luminescence based on energy deposition by secondary electrons

K. Michaelian and A. Menchaca-Rocha
Instituto de Física, Universidad Nacional Autónoma de México, Apartado Postal 20-364, 01000 México Distrito Federal, Mexico
(Received 12 October 1993)

A model is proposed to describe the production of light induced by energetic ions in scintillator materials, based on the distribution of energy deposited by the secondary electrons produced along the ion's track. The initial energy of the electrons is determined using an impulse approximation in which their motion is constrained to the radial direction, perpendicular to the ion's track. The residual energy of the electrons along the radial coordinate is obtained from an expression for the specific energy loss obtained from Lindhard's potential theory. Contributions from backscattered electrons to the energy deposition are included in the calculation. Local production of energy carriers is assumed to be proportional to the local density of deposited energy, in the absence of quenching effects. The latter are introduced by assuming the existence of a maximum energy density greater than which prompt quenching predominates and the energy carrier density reaches a maximum constant value. Light production is related to the process of energy transport through thermal diffusion of energy carriers to luminescence centers. Simple algebraic expressions are given for the energy deposition profile and for the specific luminescence. Model predictions are compared with published experimental data from various organic and inorganic scintillators.

I. INTRODUCTION

The extensive use of scintillating materials in experimental particle detection systems has motivated an important theoretical effort to understand the underlying physical processes in the production of light induced by energetic incident ions in these materials. Although a number of models[1–8] describing the luminescent response of scintillators have existed for some time, they have been almost completely ignored by experimenters using particle detection techniques based on organic and inorganic scintillation materials. In particular, the energy calibration of the light output response of these scintillators is, most often, based on an arbitrary n-parameter fit to the data, where n is usually greater than 6.

The present authors believe that this situation is due to two principal reasons. First, the quantitative models are so complex as to make their application to routine detector calibration impractical. These complexities of the existing models, based on electron energy deposition, arise from the complicated nature of the electron production cross section and low energy electron scattering and backscattering. Second, and more importantly, the models have not been demonstrated to accurately and unambiguously describe the data over a wide range of incident charges and energies without the need for ion dependent parameters.

Similarly, no uniformity has been demonstrated in describing data from both organic and inorganic scintillator materials with the same model. Part of this latter deficiency has had to do with speculation about the origin of nonlinearities in the light production process. In fact, there has been experimental evidence for some time[9,10] that the activator depletion mechanism in inorganics (a feature of many of the above referenced models) does not contribute significantly to the observed decline in scintillation efficiency at high specific energy loss. Nonradiative electron-hole (e-h) pair or exciton-exciton annihilation, and damaged molecular or crystal structures acting as electron or hole traps, collectively refered to as "quenching mechanisms" in regions of high energy deposition density, are now generally accepted[8] as being the principal causes of the observed nonlinearity.

In the present work, we determine the secondary electron energy deposition profile $\rho(r)$ by using a number of justifiable approximations which lead to a simple algebraic expression. This expression includes contributions from the backscattered electrons, commonly overlooked in luminescence models. We assume that the regional density of e-h pairs or excited molecular structures (which we define as "energy carriers"), in the absence of quenching effects, is proportional to the local energy deposition density and that the quenching is an explicit property of each particular material and one which can be determined, quantitatively, directly from the data. The assumption of proportionality of the observed light output to the quenched energy carrier density is shown to provide good fits to the experimental light versus energy data for all ions but requires a z dependence of the normalization constant for the very light ions ($z \leq 5$). For alkali halides, this dependence is removed by a simplified consideration of the process of energy transport through thermal diffusion of electrons and holes to luminescence centers or V_k centers in the lattice, which leads to detectable visible light or to partially detectable ultraviolet light, respectively. A similar, though different, process is

described for organic scintillators. Simple algebraic expressions are also obtained for the specific luminescence dL/dx. The model is compared to experimental data from a wide range of incident ions and energies and from both organic and inorganic materials with good results.

Besides providing a description of the underlying physics, the simplicity of the model makes it ideally suited to scintillation detector calibration. Other potential applications of the energy deposition part of the model include radiation therapy of tumors with ion beams, dosimetry measurements, the formation of etchable tracks in dielectrics,[11] and other experimental particle detection techniques.

II. A HISTORICAL PERSPECTIVE

In the following, we will review those models that have contributed in a general way to the scheme of our proposed model. It is in no way meant to be an exhaustive review. Reference 12 contains a good summary of the data and theoretical approaches taken before 1963.

An in depth analysis of the luminescence observed in organic crystals in response to various incident radiations was first attempted by Birks.[1] In this theory, the passage of an ionizing particle through the crystal produces a number (AdE/dx) of "excitons" (loosely defined as excited or ionized molecular structures for organic materials) proportional to the specific energy loss and also a number (BdE/dx) of damaged molecules, acting as quenching agents for the excitons, also proportional to the specific energy loss. Assuming that the light output is proportional to the effective number of excitons, the specific luminescence is thus given by

$$\frac{dL}{dx} = \frac{AdE/dx}{1 + kBdE/dx} , \tag{1}$$

where k is the exciton capture probability of a damaged molecule relative to an undamaged molecule. The values of A and kB are taken from experiment and depend on the nature of the incident particle and the medium through which it is passing. Therefore, Eq. (1) has little predictive capability and says little about the underlying physical processes.

There followed a number of attempts to describe the scintillation process from a more fundamental approach. The fact that luminescence production differed for two particles of exactly the same dE/dx but different atomic number led Meyer and Murray[2] (MM) to look for some property of the energy loss process which differs for the two particles. This property was found to be the energy distribution of the secondary scattered electrons from the ionizing collisions of the incident particle with the electrons of the stopping material. The particle with a higher z value, for the same dE/dx, will produce a more energetic spectrum of secondary electrons. Thus the density of deposited energy about the track of the ion will be less and there should be less quenching, viewed by MM as a local depletion of available activator sites (saturation), leading to a greater efficiency at producing luminescence.

In the MM model the total observed specific luminescence $(dL/dx)_t$ is composed of two parts. One part, $(dL/dx)_p$, is due to a primary column of ionization immediately surrounding the track of the ion and which is proportional only to the dE/dx of the ion. A second part, $(dL/dx)_\delta$, is due to the escape from this column of the higher energy δ rays, which would be z dependent. Therefore,

$$\left(\frac{dL}{dx}\right)_t = \left(\frac{dL}{dE}\right)_p \left(\frac{dE}{dx}\right)_p + \left(\frac{dL}{dE}\right)_\delta \left(\frac{dE}{dx}\right)_\delta . \tag{2}$$

From the NaI(Tl) experimental $(dL/dE)_t$ versus (dE/dx) data of Newman and Steigert,[13] MM derived a single (independent of the incident ion) curve for $(dL/dE)_p$ versus $(dE/dx)_p$. From other experiments,[14] they suggested that in the energy range of the electrons of the experiment (1–22 keV), $(dL/dE)_\delta$ was very nearly a constant. Making various extreme assumptions about the electron emission isotropy, they calculate limits for a universal curve of the fraction of energy $F \equiv (dE/dx)_\delta/(dE/dx)_t$ deposited outside the primary column. This fraction was found to depend only on E/A of the ion if the primary column radius is only weakly dependent on $(dE/dx)_p$. In other words, the primary column radius was assumed independent of the charge of the ion. Qualitatively their model represented the data but quantitative predictions were not possible.

There followed experimental investigations[9,10] on the validity of the activator-depletion hypothesis of quenching, showing that saturation is not an explanation of the observed decline in scintillation efficiency at high specific energy loss.

Kobetich and Katz[3] (KK) quantified the work of Murray and Meyer by determining explicitly an expression for the energy density deposited by the scattered electrons at a given radius from the ion's track. They did this by considering the following three pieces of information: the number of secondary electrons generated with a given initial energy, the residual energy of these after passing a given radial distance from the ion track, and the probability of these arriving at this radius when backscattering is considered.

The number of δ rays per unit length of the ion's track liberated from the stopping material was taken from the Mott formula[15] for elastic scattering of electrons by the Coulomb field of a nucleus. The residual energy of the electrons was calculated from the empirical relation $R = A\omega_0[1 - B/1 + C\omega_0]$, where R is the practical range of an electron of initial energy ω_0, and A, B, and C are constants valid for a range of electron energies. Because of backscattering, the low energy electrons follow a complicated route. Thus, the fraction of incident electrons that are transmitted by an absorber was taken from the empirical relation of Rao.[16]

These three ingredients were combined in the KK model to obtain an expression for the energy flux $\mathcal{W}$, carried by the δ rays through a cylindrical surface of radius r whose axis is the ion's path, which could only be solved numerically. Based on the hypothesis of local depletion of activator sites, the probability per luminescence center for the emission of a photon from a region which has absorbed a uniform energy dose of

$$\rho(r) = -\frac{d\mathcal{W}}{dA} , \tag{3}$$

where A is the area transverse to the ions track, was taken as

$$P = 1 - \exp(-\rho/\rho_0) , \tag{4}$$

where ρ_0 is the energy density required to excite 63% of the luminescence centers of the region. In spite of the experimental evidences against the argument, depletion of activation sites (saturation) was maintained as an explicit feature of this model. Comparison of the theory[3] with the experimental data of Ref. 13 for NaI(Tl) showed good results for some ions but poor fits for others.

Luntz[4] proposed a model for luminescence production in NaI(Tl) similar to Meyer and Murray[2] in which an imaginary cylinder surrounds the ion track to partition the crystal into regions of high and low energy deposition density. Luntz assumed that the scintillation efficiency dL/dE receives a negligible contribution from within the high-density region because of nonradiative events favored by high ionization density such as electron-hole recombination, radiation damage, and lattice heating effects. The luminescence response to energy deposited outside the high-density cylinder is assumed to be linearly proportional to the deposited energy. The energy deposition density for the region beyond the high-density cylinder was obtained by a survey of the numerical results of Kobetich and Katz[3] [Eq. (3)] from which they empirically deduced

$$\rho(r) = \frac{Kz^{*2}}{r^2V^2}, \tag{5}$$

where K is some constant and z^* is the effective charge of the ion. For every incident ion in the Luntz model there are two adjustable parameters, one of which determines the radius of the high-density cylinder for a given ion of charge z and velocity V, and the other which normalizes the final L versus E_0 curve (where E_0 is the incident ion energy) to the data for a given z. Comparison of the Luntz model with the data of Ref. 13 showed that the two parameters are nonlinear in z, at least over the experimental range of z to which the model was applied, and only a rough quantitative agreement with the data was found. In a later, revised version of the model[5] they considered contributions to dL/dE from the high-density region through a "linear-falloff" approach. The regional luminescence response was assumed proportional to the deposited energy density at radii greater than the "falloff" radius and fell linearly to zero contribution in a small core region in the immediate vicinity of the ion track. This core region was determined by V/f_0 where f_0 is the electron natural frequency. The beginning of the falloff is an adjustable parameter of the model. With these revisions, an improvement was claimed in the comparison with the data in the low and intermediate ion velocity regions.

Muga, Griffith, and Diksic[6,7] (MGD) have developed a model for luminescence production in thin organic films based on the formula

$$\frac{dL}{dx} = \mathcal{I}n_s\sigma \tag{6}$$

for specific luminescence in the absence of quenching-saturation effects. Here $\mathcal{I}$ is the number of electrons penetrating a thin disk, perpendicular to the track of the incident ion, of thickness dx, and n_s is the number of scintillator sites per unit volume. The cross section σ for luminescence production is taken to be a constant, independent of electron energy. Regional luminescence is therefore assumed to be proportional to the number of electrons penetrating the region and not to the regional energy deposition. To determine $\mathcal{I}$, the distribution of the scattered electrons is taken from the Rutherford scattering formula and, for simplicity, their range in the material is taken to be linearly proportional to their initial energy, i.e., $R = a\omega_0$.

Saturation effects are assumed and taken into account by supposing that there is a radius from the ion's track $r_{\rm sat}$ below which the number density of scattered electrons $\rho(r_{\rm sat})$ is greater than some critical number density $\rho_{\rm sat}$ at which all luminescence centers are excited and the light output reaches a constant maximum value. The specific luminescence is then proportional to the number density of electrons scattered through the thin disk, except in the saturation region where it is proportional to $\rho_{\rm sat}$, i.e.,

$$\frac{dL}{dx} = C\left[\pi r_{\rm sat}^2\rho_{\rm sat} + \int_{r_{\rm sat}}^{r_{\rm max}} \rho(r)2\pi r dr\right], \tag{7}$$

where C is a normalization constant. Use of the Rutherford scattering cross section leads to a complicated expression for $\rho(r)$ even when using the unjustifiable simplification that the range of an electron is linearly proportional to its initial energy. Application of the MGD model to $\Delta L/\Delta x$ data for thin NE-102 plastic scintillator[7] does quite well but only if the C factor of Eq. (7) is taken not as a constant but as a linearly increasing function of the ion charge z. MGD suggested that this empirical finding might be correcting for the fact that the cross section for luminescence production σ was taken in their model to be a constant.

In previous works[17,18] we have applied the MGD model to L versus E_0 experimental data [where L is the integral of Eq. (7) over the complete range of the ion of incident energy E_0] for thick inorganic CsI(Tl) scintillators[17] and to a procedure for calibrating these detectors.[18] Although those results were encouraging, a nonlinear C dependence on z was found. We suspected, as did Muga and Diksic,[7] that the linear dependence of the electron range on their initial energy was too gross a simplification. Also, we can see no inherent justification in assuming that the light output of a region should be proportional to the number of secondary electrons that pass through the region (i.e., a constant cross section σ for luminescence production) and not to the energy deposition density. Further, no account was taken of the effect of electron backscattering. Finally, the physical picture presented by the MGD model falsely attributes the decrease in luminescence efficiency at high dE/dx to saturation of luminescence centers.

Salamon and Ahlen[8] have taken static energy deposition models one step further by allowing e-h pairs to

migrate away from regions of high pair density and low scintillation efficiency for a time equal to the e-h pair lifetime in pure, room temperature NaI ($\sim 10^{-8}$ s). Based on some experimental evidence,[19] they assume nonradiative quenching of the e-h pairs to be proportional to the square of the pair density n. Their equation for the simultaneous diffusion and self-annihilation of the e-h pairs is then

$$\frac{\partial n}{\partial t} = D\nabla^2 n - Kn^2, \tag{8}$$

where the constants D and K, along with a constant η which describes the number of NaI molecules required to accomodate one e-h pair, are parameters to the model. Qualitative fits are obtained for the data of Newman and Steigert[13] and their own data[8] obtained for ^{20}Ne, ^{40}Ar, and ^{56}Fe from low to relativistic energies. However, the model is noted[8] as being computationaly intensive and the fits (at least for low energies where the model can be compared to data) are not more impressive than those obtained with static energy deposition models.

The following section is a derivation of our electron energy deposition model. In Sec. IV we apply the model to the production of light in scintillating materials, and in Sec. V we compare the results of the model with various experimental data.

III. THE ELECTRON ENERGY DEPOSITION MODEL

We take an approach commonly used to derive a classical expression for the specific energy loss dE/dx (the Bethe-Bloch equation). We make use of an "impulse approximation" by assuming that the collision between the incident ion and the electrons of the medium lasts for such a short time, in comparison to the inverse of the electron natural frequency, that an impulse is given to the electron without changing its position during the collision time. The electron is therefore constrained to move perpendicular to the trajectory of the ion.

To determine the magnitude of the perpendicular impulse given to an electron we consider the strength of the electric field at the site of the electron due to the heavy ion,

$$\mathcal{E} = \frac{z^* e^2}{r^2} ,$$

where z^* is the effective ion charge (less than the nominal charge z at low velocities because of electron pickup) as given by Montenegro *et al.*,[20]

$$z^* = z\left[\frac{1-\exp(-\alpha\mu)-1/6\alpha\mu\exp(-2\alpha\mu)}{1-\exp(-\mu)-1/6\mu\exp(-2\mu)}\right] , \tag{9}$$

where $\alpha = z^{-2/3}$, and $\mu = V/v_b$ with $v_b = 2.187\,69\times 10^8$ cm/s, the Bohr velocity. Equation (9) is valid for ion energies above 0.2 MeV/amu. The impulse perpendicular to the trajectory of the incident ion is then

$$\Delta p_\perp = \int_{-\infty}^{\infty} e\mathcal{E}_\perp dt = \int_{-\infty}^{\infty} e\mathcal{E}_\perp \frac{dx}{V} , \tag{10}$$

where V is the velocity of the incident ion and dx is a unit path length of the ion. Considering the electric flux Φ through an infinitely long imaginary cylinder with radius b equal to the impact parameter between the electron and the ion track, Gauss's theorem gives

$$\Phi = \int_{-\infty}^{\infty} \mathcal{E}_\perp 2\pi b dx = 4\pi z^* e. \tag{11}$$

Therefore, with Eqs. (10) and (11), we find

$$\Delta p_\perp = \frac{2z^* e^2}{bV}. \tag{12}$$

On average, the energy transfered to the electron under this impulse approximation is thus

$$\omega_0 = \frac{(\Delta p_\perp)^2}{2m_e} = \frac{2}{m_e}\left(\frac{z^* e^2}{bV}\right)^2. \tag{13}$$

We treat the scattered electrons nonrelativistically since the maximum energy transfered to them by the incident ion is well below 100 keV for the ions of interest here. In a classical elastic collision, the maximum possible momentum transfer to the stationary electron is practically equal to $2m_e V$. This implies from Eq. (12) that there exists a corresponding minimum clasical impact parameter

$$b_{\min} \sim \frac{z^* e^2}{m_e V^2}. \tag{14}$$

We now make the assumption that the practical range of the electron can be written as a simple power law of its initial energy (as suggested by experiment[21,22]) of the form

$$R = a\omega_0^n. \tag{15}$$

Substituting for the energy from Eq. (13) and solving for the impact parameter, we obtain

$$b = \frac{z^*}{V}\left(\frac{2e^4}{m_e}\right)^{1/2}\left(\frac{a}{R}\right)^{1/2n}. \tag{16}$$

The number of electrons with an impact parameter between b and $b+db$ per unit path length of the incident ion track is

$$dN(b) = 2\pi\mathcal{N} b db , \tag{17}$$

where $\mathcal{N}$ is the number of electrons per unit volume of the material,

$$\mathcal{N} = N_A \cdot \frac{Z_{\text{eff}}}{A_{\text{eff}}} \cdot \varrho \tag{18}$$

with N_A the Avagadro number and where A_{eff} and Z_{eff} are, respectively, the effective atomic mass and charge of the compound material, taken to be $Z_{\text{eff}} = \sum n_i Z_i / \sum n_i$

and $A_{\text{eff}} = \sum n_i A_i / \sum n_i$ with n_i the fraction of atoms by number of the element i in the compound, and ϱ the material density in g/cm^3.

The number of electrons that after the interaction will have a range between R and $R + dR$ is then

$$dN(R) = \frac{dN(b)}{db}\frac{db}{dR}dR = \pi\mathcal{N}\frac{2e^4}{m_e}\frac{a^{1/n}}{n}\frac{z^{*2}}{V^2}\frac{1}{R^{1+1/n}}dR \, . \tag{19}$$

In reality the scattered electron distribution is not expected to follow the form of Eq. (19) because of contributions from backscattering electrons. Large angle scatterings occur when the electrons collide with the atomic nuclei of the material. The reflection coefficient for electrons incident on a thick absorber is found experimentally to be relatively independent of the electron energy but is a monotonically increasing function of the atomic number of the absorbing material.[23,24] Using the Rutherford formula and assuming only a single electron scattering, Everhart[24] derived an expression for the number of electrons of nominal range R actually arriving at a depth r ($r \leq R$) in the material as

$$N(r, R) = N_0(R)(1 - r/R)^d \, ,$$

where $N_0(R)$ is the number of incident electrons of nominal range R. Good fits of a derived reflection coefficient are obtained with various experimental data for electrons of energy between 10 and 100 keV and for materials with atomic numbers between $Z = 5$ and $Z = 60$, if the power d is taken to be[24]

$$d = 0.045Z. \tag{20}$$

The probability of an electron of nominal range R making it to a distance r or more from the ion track can therefore be written as

$$P(r, R) = (1 - r/R)^d. \tag{21}$$

The total energy deposition density, per unit path length of the incident ion track, for electrons of all nominal ranges between r and the maximum possible range of the electrons $R_{\max}$ [where $R_{\max}$ corresponds to $b_{\min}$ through Eq. (16)] at a radius r from the ion's track is then

$$\rho(r) = -\frac{d}{dA}\int_r^{R_{\max}} P(r, R)\omega(r, R)dN(R) \, , \tag{22}$$

where $\omega(r, R)$ is the energy of an electron of nominal range R at a distance r from the ion track, and where the differentiation is with respect to the area transverse to the track. Equation (22) is just the rate of change (per unit area) of the energy flux carried by the electrons across a cylinder of radius r, which has to be equal to the energy deposition density as a function of r. This equation contains the implicit assumption that the residual energy of the backscattered electron is deposited at the radius at which it backscatters. That is, we do not consider any backward moving component of the energy flux. We may justify this by stating that, to first order, the number of electrons that backscatter out of a region should be equal to the number that backscatter into the region.

The residual energy $\omega(r, R)$ of an electron at a distance r from the ion track, is obtained by integrating the specific energy loss $d\omega/dr$ of the electron up to this radius. We write for the specific energy loss of the electron

$$-\frac{d\omega}{dr} = \frac{1}{na\omega^{(n-1)}}, \tag{23}$$

where a is a constant. The electron range-energy relation is thus

$$R = \int_{\omega_0}^{0} \frac{d\omega}{-d\omega/dr} = a\omega_0^n. \tag{24}$$

Integrating Eq. (23) from the electron's initial energy ω_0 to some intermediate energy $\omega(r, R)$ and making use of Eq. (24) we arrive at our desired expression

$$\omega(r, R) = \left(\frac{R}{a}\right)^{1/n}(1 - r/R)^{1/n}. \tag{25}$$

Assuming that the electrons' energy is of the same order or less than the K-shell ionization energy of the medium, given approximately by[24] $I_K(eV) = 11.3(Z - 1)^2$, then it is found that the average ionization potential I decreases approximately linearly with decreasing ω. The logarithmic term in the Bethe equation is then a constant and we arrive at Eq. (23) with $n = 2$. Equation (25) can then be rewritten in terms of the electrons nonrelativistic velocity to give the familiar Thomson-Whiddington law[25]

$$v^4 = v_0^4 - f\varrho r \, , \tag{26}$$

where f is a constant and ϱ is the material density. Comparison of the range-energy relation, Eq. (24), with experimental data[21,22] for electrons of energy less than 100 keV suggests, however, that this exponent ($n = 2$) is somewhat too large, the best experimental value being between 1.6 and 1.7.

Based on Lindhard's theory,[27] Kanaya and Okayama[26] started with a semi-empirical potential for the electron interacting with the target atom. They arrive at Eq. (23) with $n = 5/3$, which gives a range-energy relation that corresponds closely to experiment. In their case, the constant a is

$$a = \frac{5.025 \times 10^{-12} A_{\text{eff}}}{0.182\varrho Z_{\text{eff}}^{8/9}} \tag{27}$$

giving a range R in cm if ω_0 is in eV and where ϱ is the material density in g/cm^3 and A_{eff} and Z_{eff} are, respectively, the effective atomic mass and charge of the compound material.

Whatever the value chosen for the power n in the range-energy relation, with Eqs. (19), (21), and (25) the energy deposition density, Eq. (22), becomes

$$\rho(r) = -\pi\mathcal{N}\frac{2}{n}\frac{e^4}{m_e}\frac{z^{*2}}{V^2}\frac{1}{2\pi r} \times\frac{d}{dr}\int_r^{R_{\max}}\frac{(1-r/R)^{d+1/n}}{R}dR. \quad (28)$$

Evaluating Eq. (28), we arrive at a general expression for the electron energy deposition density per unit path length of the incident ion as a function of the radial distance r ($b_{\min} < r < R_{\max}$) from the ion's track,

$$\rho(r) = \mathcal{N}\frac{e^4}{nm_e}\frac{z^{*2}}{V^2}\frac{1}{r^2}\left[1-\frac{r}{R_{\max}}\right]^{d+1/n}, \quad (29)$$

where $d = 0.045Z_{\text{eff}}$. From Eq. (14) and (16) we find $R_{\max} \sim a(2m_e)^n V^{2n}$. It is interesting to note that except for the additional term in square brackets, this expression [Eq. (29)] is equivalent to that used by Luntz[4] [see Eq. (5)] which was obtained by direct comparison with numerical calculations of Kobetich and Katz[3] based on Eq. (3). The importance of the portion $(1-r/R_{\max})^d$ of the additional term in square brackets increases as the Z_{eff} of the medium increases and can be attributed to the effect of electron backscattering. Equation (29) is plotted, for the choice $n = 5/3$ in Fig. 1 for the ions ^{16}O and ^{40}Ca at 100 MeV incident on organic CH and inorganic NaI and CsI materials.

IV. APPLICATION TO A LUMINESCENCE MODEL

The regional density of e-h pairs or excited molecular structures (energy carriers) created in the scintillator material is assumed to be proportional to the energy deposition density. It has, for example, been verified experimentally[28] that the secondary electron yield at the surface of a material is directly proportional to the energy deposition density at the surface. Quenching effects (see Refs. 8 and 12 for a review) are included without yet specifying their nature (certainly different for organics than for inorganics) by considering that there is a maximum energy deposition density ρ_q greater than which the energy carrier density remains at a constant maximum value.

The quenching density ρ_q is an inherent constant of the scintillator material. Its value can be determined by obtaining a best fit of the model generated L versus E_0 (where E_0 is the ion incident energy) curve with the equivalent experimental curve, while varying ρ_q, for only one ion. The distance from the incident ions track r_q at which the energy deposition density falls below the quenching density can be calculated through an iterative procedure (the Newton method found to be the most appropriate) from Eq. (29) with $\rho(r)$ replaced by ρ_q. The specific (per unit path length of the ion) quenched energy carrier density is then

$$\frac{dN_e}{dx} = K\left[\pi r_q^2\rho_q + \int_{r_q}^{R_{\max}}\rho(r)2\pi r dr\right], \quad (30)$$

where K is the constant relating the energy deposited to the number of energy carriers formed. We next assume that the regional light output is proportional to the regional energy carrier density (this point will be discussed in more detail below) giving

$$\frac{dL}{dx} = C\frac{dN_e}{dx}, \quad (31)$$

where C is an overall normalization constant including the constant K, experimental gains, and a constant of proportionality relating the energy carrier density to light output. It might be argued that Eq. (30) is somewhat unphysical because of the discontinuity in the contribu-

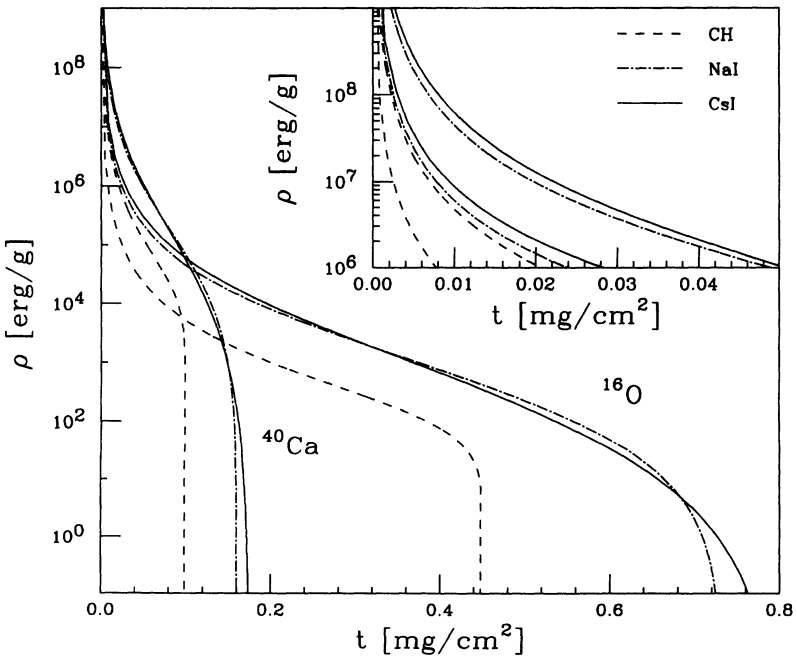

FIG. 1. The electron energy deposition density as a function of the radial thickness $t = r\varrho$ from the ion track for $^{16}_{8}$O and $^{40}_{20}$Ca at 100 MeV on organic CH and inorganic NaI and CsI materials.

tion at the quenching radius r_q. Reaching a maximum constant value for the regional light output is perhaps an idealization but it is in agreement with observed behavior and with the Birks formulation of Eq. (1). A more continuous approach, in complete accord with the Birks formulation and with experiments[12] observing the degradation of luminescence efficiency in organic materials with high dose γ-ray and electron irradiation, would be

$$\frac{dL}{dx} = C \int_{b_{\min}}^{R_{\max}} \frac{\rho(r)}{1+\rho(r)/\rho_q} 2\pi r dr. \tag{32}$$

It was found, however, that this approach leads to only a very slight improvement in the comparison of the theory to the data, at the expense of not being able to carry out the integration analytically. As an alternative approach, we have also tried the assumption incorporated in the original model of Luntz[4] that the light output receives a negligible contribution from a high-density region surrounding the track because of competition from nonradiative events. However, in all cases, this gave worse fits to the data than the assumption of a maximum constant contribution. We therefore retain Eq. (30) as adequately representing the quenching process.

The integral of Eq. (30) can most easily be carried out analytically if the power $d + 1/n$ in Eq. (29) for ρ is a simple rational number. We take $n = 5/3$ and find that for the scintillator CsI, $Z_{\text{eff}} = 54$ giving $d + 1/n = 3.03 \approx 3$. For the scintillator NaI, $Z_{\text{eff}} = 32$ giving $d + 1/n = 2.04 \approx 2$ and for the plastic scintillator material CH, $Z_{\text{eff}} = 3.5$ giving $d + 1/n = 0.7575 \approx 3/4$. Substituting for ρ_q and $\rho(r)$ from Eq. (29) and carrying out the integral in Eq. (30), we arrive at, for CsI,

$$\frac{dL}{dx} = \pi C \mathcal{N} \frac{6}{5} \frac{e^4}{m_e} \frac{z^{*2}}{V^2} \left[\frac{1}{6}\mathcal{R}^3 - \frac{1}{2}\mathcal{R}^2 - \mathcal{R} - \ln(1-\mathcal{R}) \right], \tag{33}$$

with $\mathcal{R} = (1 - r_q/R_{\max})$, which can be interpreted as the fraction of the total radial extent of the energy deposition region which lies in the nonquenched region. For NaI,

$$\frac{dL}{dx} = \pi C \mathcal{N} \frac{6}{5} \frac{e^4}{m_e} \frac{z^{*2}}{V^2} \left[-\mathcal{R} - \ln(1-\mathcal{R}) \right], \tag{34}$$

and for plastic CH,

$$\frac{dL}{dx} = \pi C \mathcal{N} \frac{6}{5} \frac{e^4}{m_e} \frac{z^{*2}}{V^2} \left[-\frac{5}{6}\mathcal{R}^{3/4} + \ln\left(\frac{1+\mathcal{R}^{1/4}}{1-\mathcal{R}^{1/4}}\right) - 2\tan^{-1}\mathcal{R}^{1/4} \right]. \tag{35}$$

The total light output response of a thick scintillator induced by a stopped ion of incident energy E_0 can be obtained by summing the appropriate equation [(33) – (35)] over small finite segments Δx of the ion's range. The ion's energy loss in each finite segment can be obtained from the Bragg rule for the stopping power of a composite medium

$$S = \sum_i w_i S_i, \tag{36}$$

where $S = 1/\varrho(dE/dx)$ and w_i is the fraction by weight of the atom i in the medium. The stopping power S^z of an ion of nominal charge z can[29] be given in terms of the stopping power of a proton S^p in the same material by

$$S^z(E) = z^{*2} S^p(E/A), \tag{37}$$

where z^* is the effective charge [Eq. (9)] and where A is the mass number of the ion. For an energy per nucleon E/A of the ion between 10^3 and 10^5 keV/amu, we have used the parametrization of Ref. 29,

$$S^p(E/A) = 602.204 A \frac{a_1}{\beta^2} \ln\left[\frac{a_2\beta^2}{1-\beta^2} - \beta^2 - \sum_{j=0}^{4} a_{j+3}[\ln(E/A)]^j \right], \tag{38}$$

in MeV/(g/cm^2) with the constants a_j, as listed in the same reference, dependent on the material.

V. RESULTS

Before comparing our results directly with experimental data, we point out a number of interesting features which follow directly from the model. The model-determined scintillation efficiency dL/dE versus ion velocity V is plotted in Fig. 2 for those ions included in the data set of Colonna *et al.*[30] From the figure, it can be seen that at a fixed velocity, the lower z ions are more efficient at producing luminescence. As the velocity increases the efficiency tends to reach a constant maximum value. This is due to the fact that with increasing velocity a greater portion of the energy lost by the ion gets deposited outside of the quenching region and so light production becomes more nearly proportional to the energy deposited. The inset of the figure shows the fraction F of the energy lost by the incident ion deposited outside of the quenching region as a function of the ion's velocity. For a given velocity (or E/A) this fraction is a function of the ion's charge, but not a very strong one for the heavier ions. Figure 2 also demonstrates the well-known and previously explained[2] fact that lower mass isotopes at a given energy are more efficient at producing light than higher mass ones. At a given energy the lower mass isotope has a larger velocity and thus the fraction of deposited energy outside the quenching region is larger and hence the luminescence efficiency is larger. The observed differences are accurately reproduced by our model, as will be demonstrated below.

The assumption of Meyer and Murray (see Sec. II or Ref. 2) that the fraction of energy deposited outside the "primary column" is independent of the ion charge is equivalent to the reduction of all individual ion curves in the inset of Fig. 2 to a single, average curve. In view of the excellent fits of our model to the data (demonstrated below) this is clearly an over simplification. The

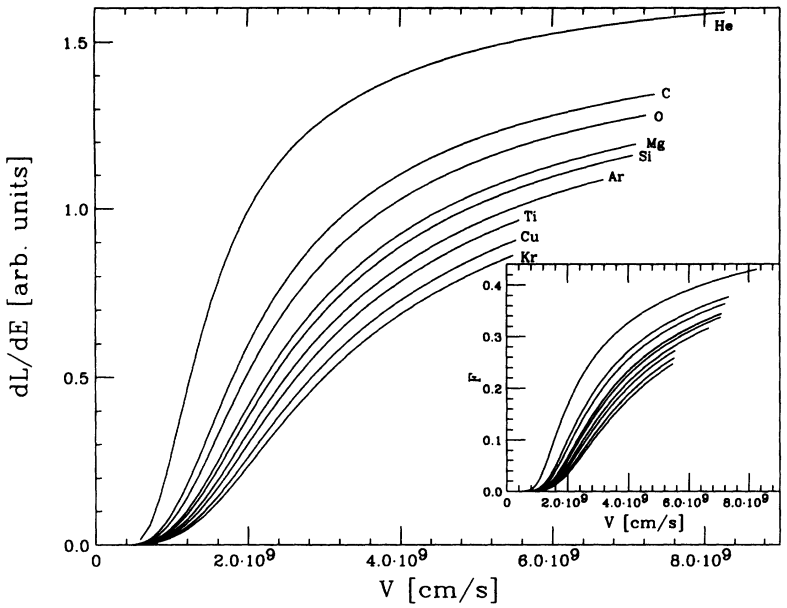

FIG. 2. Scintillation efficiency dL/dE versus ion velocity, as determined by the model, for the ions included in the data set of Colonna *et al.* (Ref. 30). The curves were obtained with the quenching density $\rho_q = 8.9 \times 10^6$ erg/g and the exponent $n = 5/3$ in the range-energy relation. The inset shows the fraction of the total energy deposited outside of the quenching region as a function of the ion's velocity.

assumption of Luntz, in their original model,[4] that the energy deposited inside the "high-density" region has a negligible contribution to the luminescence is equivalent to taking the luminescence efficiency proportional to the curves in the inset of the figure, i.e., to F, and not to the curves of the main figure.

The model-generated luminescence efficiency dL/dE as a function of the ion energy loss dE/dx is plotted in Fig. 3 for the ions included in the data set of Colonna *et al.* The observed rapid decrease in scintillation efficiency with energy loss is again related to the energy sharing between quenched and nonquenched regions. For a given dE/dx, the curves of the figure are double valued in luminescence efficiency. This is because as the ion slows down its energy loss increases until its velocity is close to that of the atomic electrons in the material, at which point the ion starts to pick up electrons, decreasing its effective charge and hence also its energy loss. The luminescence efficiency continues to decrease because the fraction F of energy deposited outside the quenching region is a monotonically decreasing function with decreasing ion velocity.

For ion energies above that corresponding to the maximum in dE/dx, it can be seen from Fig. 3 that the ion with a higher z value is more efficient at producing light. This is due to the fact that to have the same dE/dx as a lower z ion, the higher z particle must have a higher velocity. Since, as demonstrated in the inset of Fig. 2, the fraction of energy that is deposited outside the quenching region is a stronger function of velocity than of ion charge, for a given dE/dx the higher z ion must be more efficient at producing light.

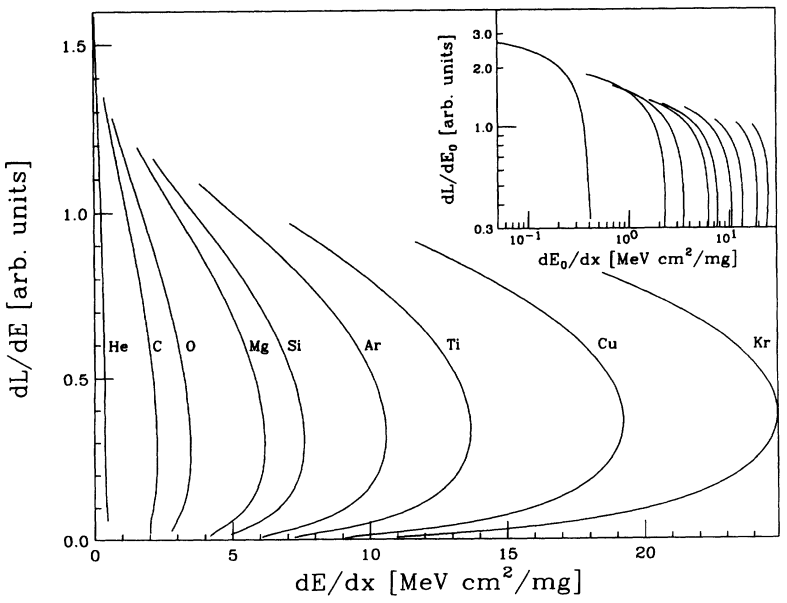

FIG. 3. The model-generated scintillation efficiency dL/dE [obtained from $(dL/dx)/(dE/dx)$] as a function of the ion's specific energy loss for the ions included in the data set of Colonna *et al.* (Ref. 30). The curves were obtained with the quenching density $\rho_q = 8.9 \times 10^6$ erg/g and the exponent $n = 5/3$ in the range-energy relation. The inset shows the differential efficiency dL/dE_0 (see text) plotted on a log-log scale for direct comparison with the experimental data of Colonna *et al.* (Ref. 30). The labeling of the ions in the inset follows the same ordering as in the main plot.

No strong onset of a plateau is observed in the luminescence efficiency as the ion's energy loss decreases with increasing energy. On the contrary, the efficiency continues to increase with decreasing dE/dx. For comparison with traditional analyses, the inset of the figure shows the differential efficiency dL/dE_0 (the slope of the model generated L versus E_0 curve, where E_0 is the incident energy) as a function of the ion's energy loss dE_0/dx at incident energy. Plotted on a log-log scale, these curves can be directly compared with analyses of the experimental data (see Colonna *et al.*[30]).

Figure 4 shows the experimental data points of Ref. 7 for the specific luminescence $\Delta L/\Delta x$ as a function of incident energy per nucleon E_0/A for various incident ions on a thin film organic (plastic NE-102) scintillator. The curves were obtained directly from Eq. (35). The quenching energy deposition density ρ_q (in erg/g), as determined by obtaining a best fit of the theory to the data, is listed on the figure. The trends of the data are well reproduced by the model; the curves lie well within the experimental error bars of all points. The inset of Fig. 4 shows the normalization constant C of Eq. (35) needed to obtain the best fit of each theoretical curve with the experimental data, as a function of the incident ion charge z. The individual values are expressed as a percent difference of the average C value of the data set. It can be seen that, in contrast to the results obtained by Muga and Diksic,[7] no arbitrary $C(z)$ correction factor is needed since all C values vary by not much more than 10% of the average value and this variation is within the experimental error bars (drawn for a few representative points on the plot).

Figure 5 shows the experimental light response (L versus E_0) for ions stopped in thick CsI(Tl) scintillator for the published data of Colonna *et al.*[30] The solid lines are the model generated light response curves obtained with Eqs. (33) and (36). The inset shows the normalization (C versus z) curve. The values are in a percent difference from the average of all C values for the data set.

Figure 6 shows the data of Newman and Steigert[13] (after subtraction of a common luminescence pedestal of 0.2 and digitizing the continuous data curves presented in the reference) taken with ions stopped in a thick NaI(Tl) scintillator. The model curves were obtained directly from Eqs. (34) and (36). The poorer fits of the model at lower ion energies is probably related to experimental errors in determining the energy of the degraded beam due to imprecise energy loss tables existing at the time of the experiment. We include this older data set as it provides a benchmark for comparison of our model with previous theoretical calculations. To be noted are the accurate predictions of the model for the two isotopes ^{10}B and ^{11}B. The best fit normalization constant, C, is the same for both isotopes.

Figure 7 shows the experimental data of Buenerd *et al.*[31] and model generated curves obtained with Eq. (35) for ions stopped in a thick Pilot U plastic scintillator.

A number of experimental effects may be imagined which could lead to the dependence of the normalization constant C on z found for the $z \leq 5$ ions (insets in Figs. 5–7). These include (1) the variation of the light collection efficiency as a function of the different particle ranges in a given detector due to transmission losses at the surfaces and absorption losses in the scintillating material; (2) incident surface quenching due to escape of energy carriers and surface impurities acting as energy carrier traps;[12] (3) the pulse shape dependence on dE/dx, especially for organics and CsI(Tl), in relation to finite width time gates and phototube-diode sensitivities to the shape of luminescence spectrum, which is known to depend on the ion charge z and the activator concentration;[9] (4) ion channeling effects in inorganic scintillators.[5] However, for example, none of these alone or taken together can account for the strong dependence found of C on z for the low z ions of the data of Colonna *et al.*[30] (Fig. 5). Instead, we believe that a consideration

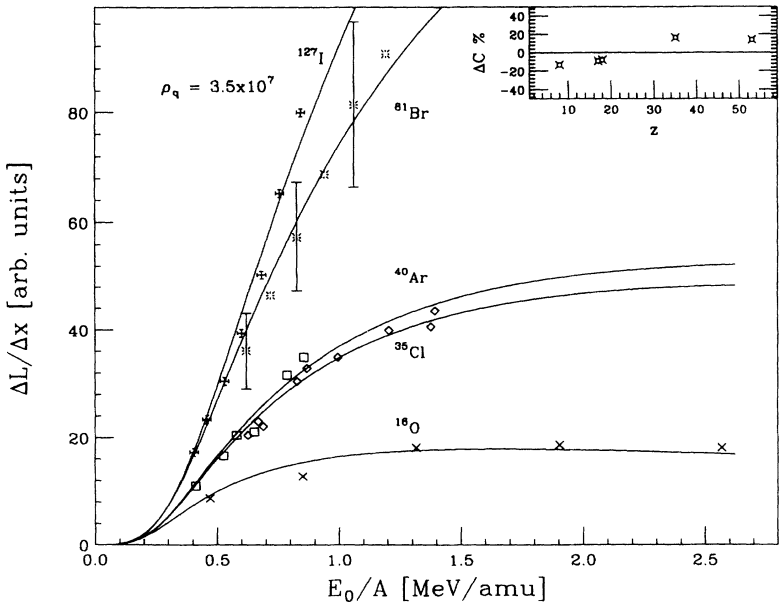

FIG. 4. The specific luminescence as a function of incident energy per nucleon of various ions on a thin film organic (plastic NE-102) scintillator. The experimental data points were taken from Ref. 7 and the solid curves were obtained by Eq. (35). Typical experimental errors are listed for one ion only. The inset shows the normalization constants, as a percent difference from the average value, needed to obtain a best fit of each theoretical curve with the corresponding data. ρ_q is the quenching density (in ergs/g) chosen.

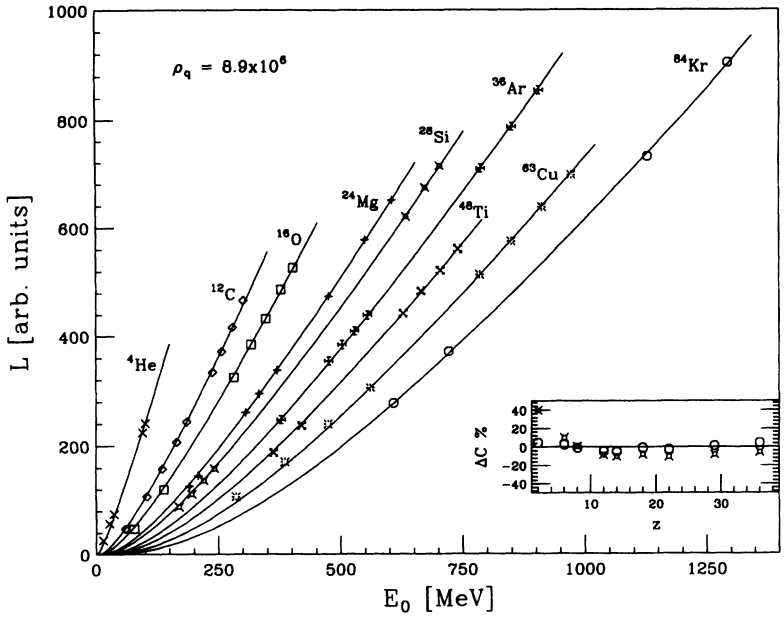

FIG. 5. A comparison of the calculated light output response (L versus the incident energy E_0) curves (solid lines) for various ions with the experimental data of Colonna *et al.* (Ref. 30) taken with a thick CsI(Tl) scintillator. The crosses in the inset show the normalization constants, as a percent difference from the average value, needed to obtain a best fit of each theoretical curve with the corresponding data. The circles in the inset show the variation of the normalization constants obtained with an extension of the model to include the electron and hole diffusion process (see text).

of the process of the transport of energy from the location of charge carrier production to luminescence centers could provide an explanation. The luminescence process can thus be divided up into two parts, a prompt energy quenching part depending explicitly on the shape of the energy deposition density, to which the model has so far been addressed, and a slower part including the thermal diffusion of the energy carriers and competition between their nonradiative annihilation or radiative recombination at luminescence centers.

For the inorganic alkali halide materials, prompt quenching of the energy carrier density can be considered as a competition between nonradiative recombination of electrons and holes and electron capture at activator impurity sites which at a later time become available for light production. In fact, such a description leads directly to Eq. (32) with $\rho_q = \mathcal{D}\rho_a$ where $\mathcal{D}$ is a constant and ρ_a is the activator density.[34]

We now turn our attention to the energy transport part of luminescence production giving only a brief summary for the alkali halide CsI(Tl), more details can be found in Refs. 32–34. The prompt quenching process mentioned above then leads to most of the unquenched electrons being held at Tl^+ traps (forming Tl^o) and the unquenched holes being self-trapped in the CsI lattice, forming molecular bonds between two iodide atoms, known as V_k centers. The electrons can be thermally released from the Tl^+ traps and the V_k centers can be thermally excited to the conduction band. Thermal diffusion of these charge carriers then proceeds leading to a more or less homoge-

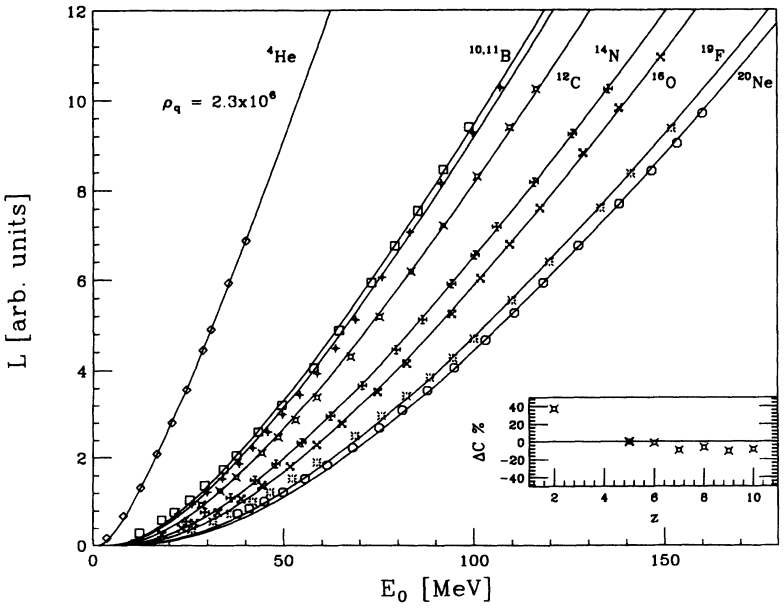

FIG. 6. A comparison of the calculated light output response (L versus the incident energy E_0) curves (solid lines) for various ions with the experimental data of Newman and Steigert (Ref. 13) taken with a thick NaI(Tl) scintillator. A common pedestal value of 0.2 has been subtracted from all experimental L values. The inset shows the normalization constants, as a percent difference from the average value, needed to obtain a best fit of each theoretical curve with the corresponding data.

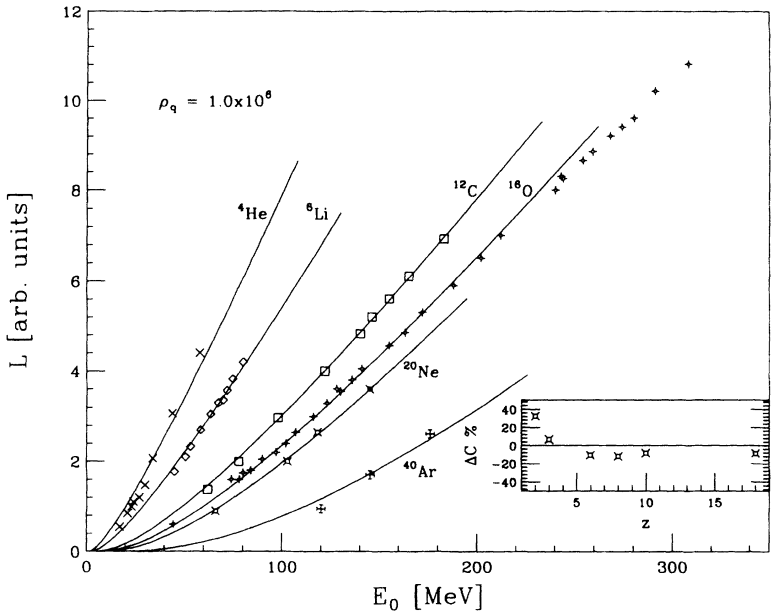

FIG. 7. A comparison of the calculated light output response (L versus the incident energy E_0) curves (solid lines) for various ions with the experimental data of Buenerd *et al.* (Ref. 31) taken with the thick plastic scintillator Pilot-U. The inset shows the normalization constants, as a percent difference from the average value, needed to obtain a best fit of each theoretical curve with the corresponding data.

neous distribution of electrons, V_k centers, and Tl sites. Next, we consider the competition between two forms of electron-hole recombination, those occurring at Tl sites giving rise to characteristic 565 nm wavelength observable light, and electron recombination with V_k centers producing no light or ultraviolet light of about 330 nm wavelength. The ultraviolet light is strongly absorbed by the Tl^+ atoms in the crystal[33] which then reemit a fraction in a broad spectrum centered at 565 nm. If we now assume that the number of recombinations at Tl sites is proportional to the density of Tl activator sites ρ_a and that the number of recombinations at V_k centers is proportional to the density of holes remaining after prompt quenching (proportional to the energy carrier density dN_e/dx) then the total observable light (565 nm band) emitted per unit path length of the incident ion would be

$$\frac{dL}{dx} = C\frac{dN_e}{dx}\left(1 - \mathcal{F}\frac{\frac{1}{K}\frac{dN_e}{dx}}{\mathcal{E}\rho_a + \frac{1}{K}\frac{dN_e}{dx}}\right), \tag{39}$$

where $\mathcal{E}$ is a constant and $\mathcal{F}$ is the fraction of the electron-V_k center recombinations that produced no light or ultraviolet light which was not reemitted in the observable region. Because of the strong absorption of the ultraviolet light, the fraction $\mathcal{F}$ should be independent of the thickness and of the Tl concentration for typical detectors. The constants $\mathcal{D}$, $\mathcal{E}$, and $\mathcal{F}$ are thus true constants of the particular type of material, in this case CsI(Tl), independent of the amount of Tl in the crystal.

Applying Eq. (39) together with Eq. (30) [in the algebraic form of Eq. (33)] to the CsI(Tl) data of Colonna *et al.* (Fig. 5), and varying $\mathcal{D}$, $\mathcal{E}$, and $\mathcal{F}$ to obtain a best fit yields $\rho_q = \mathcal{D}\rho_a = 8.9 \times 10^6$ [consistent with that obtained solely with Eq. (31)], $\mathcal{E}\rho_a = 9.0 \times 10^{-4}$ and $\mathcal{F} = 0.4$. The circles in the inset of Fig. 5 show the effect of this extension of the model. The dependence of the normalization constant on z has been removed and it is found (not shown) that the fits of the model-generated curves to the data are even better than those presented in the main figure. Assuming a nominal activator concentration for the detector of $\rho_a = 0.1$ mol% gives $\mathcal{D} = 8.9 \times 10^7$ per mol% Tl and $\mathcal{E} = 9.0 \times 10^{-3}$ per mol% Tl.

If one accepts this description of the light production process in alkali halides, then it is emphasized that there are *no* free parameters in the model except for an overall normalization constant. The constants $\mathcal{D}$, $\mathcal{E}$, and $\mathcal{F}$ should apply equally well to any CsI(Tl) detector, and only the concentration of activator sites ρ_a must be known. As a test of this hypothesis, we apply Eq. (39) with the above-determined values of the constants $\mathcal{D}$, $\mathcal{E}$, and $\mathcal{F}$ to CsI(Tl) data of Horn *et al.*[35] (also 0.1 mol% Tl). The results are shown in Fig. 8. The best ρ_q value is indeed found to be 8.9×10^6 erg/g and there is no dependence of C on z.

Although the above description of the energy transport process was specific to CsI(Tl), a very analagous situation exists for NaI(Tl).[36] For plastic scintillators, prompt quenching has been attributed to ionized or excited molecules acting as exciton traps for unimolecular, bimolecular, or j-molecular deexcitation without radiation.[12] Energy transport from the solvent to the organic scintillator also plays a role. Fast flourescence is thought to arise from deexcitation of a singlet (spin-0) excited state. A slow component to the light arises from excitation of long-lived triplet (spin-1) states. Two such excited triplet state molecules can interact leading to one molecule in the ground state and the other in the normal singlet state which quickly flouresces to the ground state. Since light from the triplet state requires a bimolecular interaction, the relative amount of light emitted in the slow portion increases as the dE/dx of the ion increases. Competition for exciton energy between the fast and slow processes could thus explain the dependence of C on z for the low z ions in the data of Buenerd *et al.* (Fig. 7) be-

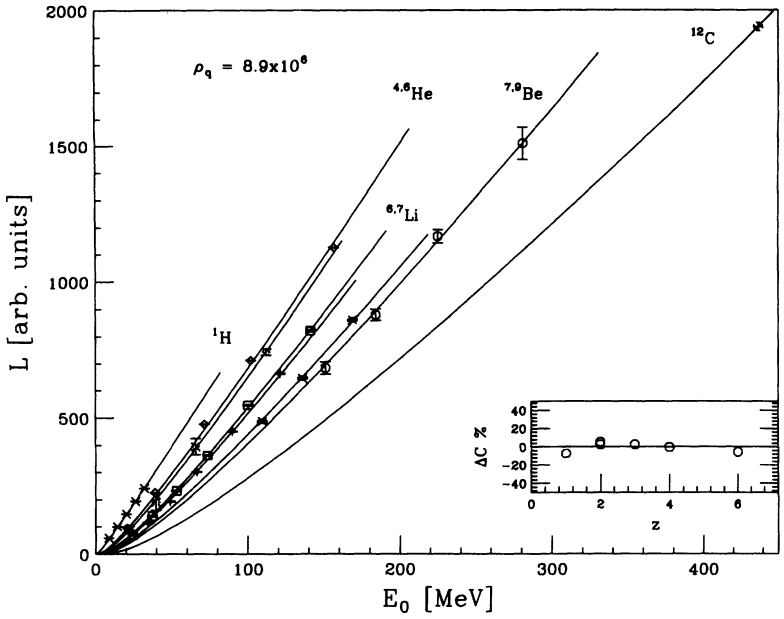

FIG. 8. A comparison of the calculated light output response (L versus the incident energy E_0) curves (solid lines) for various ions with the experimental data of Horn *et al.* (Ref. 35) taken with the thick CsI(Tl) scintillator. The curves were obtained with Eq. (39) with the same constants $\mathcal{D}$, $\mathcal{E}$, and $\mathcal{F}$ used for the data of Colonna *et al.* (circles in the inset of Fig. 5). The inset shows the normalization constants, as a percent difference from the average value, needed to obtain a best fit of each theoretical curve with the corresponding data. It is noted that the normalization constants for the different isotopes are practically identical.

cause the time gates on the light pulses for organic scintillators are normally much shorter than the time typically required to collect all of the slow component[12] and the energy-to-light conversion efficiency is less for the slow component. This process for organic scintillators is in many ways similar to that for the alkali halides but in some sense more complicated as the time dependence is normally important.

VI. CONCLUSION

We have presented a model for the production of luminescence in scintillator materials based on a calculation of the energy deposition density due to the secondary scattered electrons around the track of an energetic incident ion. By using an impulse approximation in which the motion of the electrons is confined to the radial direction, we arrive at a simple algebraic expression for the distribution of the density of deposited energy $\rho(r)$ which includes contributions from backscattered electrons. In the absence of quenching, the energy carrier density of a given region of scintillating material was assumed to be proportional to this energy deposition. In the quenching region, the energy carrier density reaches a constant maximum value. The radius of the quenching region is determined by a critical energy deposition density ρ_q. For the alkali halides, ρ_q can be related to the concentration of activator atoms and the light output is determined by a competition for electron-hole recombination at these activator sites and recombination at self-trapped holes. For the organic scintillators, ρ_q is left as the free parameter of the model and the light output is determined by the quenched exciton density. We are presently working on an extension of our model for organics, considering the two types of excitons (singlet and triplet states) and their deexcitation time dependence, which possibly will eliminate the need for the free parameter ρ_q and also remove the C of z dependence for the low z ions.

The fundamental variables characterizing the luminescent response of the ion-medium interaction were found to be the velocity V and effective charge z^* of the incident ion and the effective charge Z_{eff}, mass A_{eff}, mass density ϱ, and the quenching energy density ρ_q of the medium. For the alkali halides, ρ_q is proportional to the activator concentration ρ_a while the material constants $\mathcal{E}$ and $\mathcal{F}$ characterizing the energy-to-light conversion process are independent of ρ_a.

The principal improvements of the proposed model over existing models are a simple algebraic expression for the specific luminescence dL/dx with at most only one free parameter ρ_q; inclusion of electron backscattering; and the model's "universality," as demonstrated by the quality of the fits to the data from both organic and inorganic luminescent materials for a wide range of incident ions and energies. The authors suggest that the simplicity of the proposed model should make it a valuable tool for the energy calibration of the light output response of detectors based on the scintillation process.

ACKNOWLEDGMENTS

The authors would like to acknowledge helpful discussions with Dr. E. Belmont-Moreno and Dr. J. M. Hernández and would like to thank A. Salinas and Dr. M. E. Brandan for their interest in this work. Support of DGAPA-UNAM, Grant No. IN-100193-IF, is also gratefully acknowledged.

[1]J.B. Birks, Phys. Rev. **86**, 569 (1952).
[2]A. Meyer and R.B. Murray, Phys. Rev. **128**, 98 (1962).
[3]E.J. Kobetich and R. Katz, Phys. Rev. **170**, 391 (1968); **170**, 397 (1968).
[4]M. Luntz, Phys. Rev. B **4**, 2857 (1971).
[5]M. Luntz and G.M. Heymsfield, Phys. Rev. B **6**, 2530 (1972).
[6]L. Muga and G. Griffith, Phys. Rev. B **9**, 3639 (1974).
[7]L. Muga and M. Diksic, Nucl. Instrum. Methods **122**, 553 (1974).
[8]M.H. Salamon and S.P. Ahlen, Phys. Rev. B **24**, 5026 (1981).
[9]R. Gwin and R.B. Murray, Phys. Rev. **131**, 501 (1963).
[10]J.W. Blue and D.C. Liu, IRE Trans. Nucl. Sci. **9**, 48 (1962).
[11]R. Katz and E.J. Kobetich, Phys. Rev. **170**, 401 (1968).
[12]J.B. Birks, *Theory and Practice of Scintillation Counting* (Pergamon, New York, 1964).
[13]E. Newman and F.E. Steigert, Phys. Rev. **118**, 1575 (1960).
[14]C.D. Zerby, A. Meyer, and R.B. Murray, Nucl. Instrum. Methods **12**, 115 (1961).
[15]N.F. Mott, Proc. R. Soc. **124**, 425 (1929).
[16]B.N.S. Rao, Nucl. Instrum. Methods **25**, 261 (1964).
[17]E. Belmont-Moreno, A. Menchaca-Rocha, and K. Michaelian, Nucl. Instrum. Methods A **332**, 202 (1993).
[18]K. Michaelian, A. Menchaca-Rocha, and E. Belmont-Moreno, Nucl. Instrum. Methods A **334**, 457 (1993).
[19]N.A. Tolstoi and A.P. Abramov, Opt. Spectrosc. **20**, 273 (1966).
[20]E.C. Montenegro, S.A. Cruz, and C. Vargas-Aburto, Phys. Lett. **92A**, 195 (1982).
[21]R.O. Lane and D.J. Zaffarano, Phys. Rev. **94**, 960 (1954).
[22]L. Katz and A.S. Penfold, Rev. Mod. Phys. **24**, 28 (1952).
[23]H. Kanter, Phys. Rev. **121**, 681 (1961).
[24]T.E. Everhart, J. Appl. Phys. **31**, 1483 (1960).
[25]J.J. Thomson, *Conduction of Electricity Through Gases* (Cambridge University Press, Cambridge, England, 1906).
[26]K. Kanaya and S. Okayama, J. Phys. D **5**, 43 (1972).
[27]J. Lindhard, M. Scharff, and H.E. Schiott, Math.-Fys. Meddr. **33**, 1 (1963).
[28]H. Kanter, Phys. Rev. **121**, 677 (1961).
[29]J.R. Bird and J.S. Williams, *Ion Beams for Materials Analysis* (Academic, Sydney, Australia, 1989).
[30]N. Colonna, G.J. Wozniak, A. Veeck, W. Skulski, G.W. Goth, L. Manduci, P.M. Milazzo, and P.F. Mastinu, Nucl. Instrum. Methods A **321**, 529 (1992).
[31]M. Buenerd, D.L. Hendrie, U. Jahnke, J. Mahoney, A. Menchaca-Rocha, C. Olmer, and D.K. Scott, Nucl. Instrum. Methods **136**, 173 (1976).
[32]R.G. Kaufman, W.B. Hadley, and H.N. Hersh, IEEE Trans. Nucl. Sci. **NS-17**, 82 (1970).
[33]R.B. Murray, IEEE Trans. Nucl. Sci. **NS-22**, 54 (1975).
[34]K. Michaelian, E. Belmont-Moreno, A. Menchaca-Rocha, and J.M. Hernández (unpublished).
[35]D. Horn, G.C. Ball, A. Galindo-Uribarri, E. Hagberg, R.B. Walker, R. Laforest, and J. Pouliot, Nucl. Instrum. Methods **A 320**, 273 (1992).
[36]R. Gwin and R.B. Murray, Phys. Rev. **131**, 508 (1963).